



Published in final edited form as:

Anal Chem. 2009 February 1; 81(3): 1162–1168. doi:10.1021/ac802579z.

Microfluidic perfusion system for automated delivery of temporal gradients to islets of Langerhans

Xinyu Zhang and Michael G. Roper*

Department of Chemistry and Biochemistry, Florida State University, 95 Chieftan Way, Tallahassee, FL 32306

Abstract

A microfluidic perfusion system was developed for automated delivery of stimulant waveforms to cells within the device. The 3-layer glass/polymer device contained two pneumatic pumps, a 12 cm mixing channel, and a 0.2 μL cell chamber. By altering the flow rate ratio of the pumps, a series of output concentrations could be produced while a constant $1.43 \pm 0.07 \mu\text{L}/\text{min}$ flow rate was maintained. The output concentrations could be changed in time producing step gradients and other waveforms, such as sine and triangle waves, at different amplitudes and frequencies. Waveforms were analyzed by comparing the amplitude of output waveforms to the amplitude of theoretical waveforms. Below a frequency of 0.0098 Hz, the output waveforms had less than 20% difference than input waveforms. To reduce backflow of solutions into the pumps, the operational sequence of the valving program was modified as well as differential etching of the valve seat depths. These modifications reduced backflow to the point that it was not detected. Gradients in glucose levels were applied in this work to stimulate single islets of Langerhans. Glucose gradients between 3 and 20 mM brought clear and intense oscillations of intracellular $[\text{Ca}^{2+}]$ indicating the system will be useful in future studies of cellular physiology.

Keywords

microfluidic; perfusion; temporal; gradient; islets of Langerhans

Introduction

Defective insulin secretion from islets of Langerhans is one hallmark of type 2 diabetes, and the mechanisms by which this process becomes disrupted are unknown. The accepted hypothesis of glucose-stimulated insulin secretion involves metabolism of the sugar leading to, through a series of steps, an increase in intracellular $[\text{Ca}^{2+}]$ ($[\text{Ca}^{2+}]_i$), followed by release of insulin. While this conventional view of glucose-stimulated insulin secretion is well accepted, there are several aspects still under investigation. For example, exposure of islets of Langerhans or whole pancreas to constant concentrations of glucose results in oscillations of metabolism and oxygen consumption^{1–4}, membrane potential⁵, $[\text{Ca}^{2+}]_i$ ^{3,5,6}, and insulin secretion⁶ with periods ranging from several seconds to several minutes. These oscillations are of great interest as type 2 diabetics are known to have altered periods and amplitudes of insulin secretory oscillations as compared to non-diabetics^{7,8}. The mechanism driving these oscillations are still unclear, but testing of the various hypotheses would be facilitated by a method to accurately control the islet environment, such as by producing time-varying glucose

*Address Correspondence to: Dr. Michael G. Roper, Department of Chemistry and Biochemistry, Florida State University, 95 Chieftan Way, Dittmer Building, Tallahassee, FL 32306, Ph 850-644-1846, Fx 850-644-8281, E-mail: E-mail: roper@chem.fsu.edu.

concentrations, with a high degree of automation while still allowing the measurement of other physiological parameters such as $[Ca^{2+}]_i$ or insulin secretion.

Microfluidic devices are a popular choice for maintaining or modulating the extracellular environment of cells. Recently, there have been a number of methods developed that could enable modulation of the extracellular environment by producing a concentration gradient across a channel width^{9–14}; however, these types of gradients are not used as often as gradients in the time dimension when studying islet physiology. For example, step changes or periodic changes in glucose concentration are more common waveforms to induce $[Ca^{2+}]_i$ changes and/or initiate insulin secretion from islets.

There have been several reports of measuring $[Ca^{2+}]_i$ and insulin secretion on microfluidic devices using step-changes in glucose concentration.^{15,16} However, the perfusion systems were not fully automated, relying on either off-chip gas cylinders¹⁵ or variations in fluid height in the perfusion reservoirs¹⁶ to generate flow. A further limitation of these devices was that only a single concentration of glucose could be applied unless the solutions were manually replaced. Nevertheless, these methods have provided insight into islet physiology and have provided a framework for how a more automated perfusion system capable of producing multiple concentration profiles would be beneficial.

Pulse code modulation can be used to produce time-varying concentrations of reagents in an automated fashion.¹⁷ In this technique, off-chip pumps deliver solute and solvent to a microfluidic device. A series of valves pulse the stream of solute and solvent at specified durations and duty cycles into a mixing channel where longitudinal diffusion then smooths the pulses into a single output concentration. While this type of device has been used to generate signals such as sawtooth and cosine waveforms, the microfluidic device is complex requiring multiple input streams to ensure a high resolution between output concentrations. Flow-encoded switching of multiple sample streams is another method to produce time-varying output concentrations.¹⁸ By adjusting the flow ratio of two different sample streams (a sample and diluent), square waves of different durations can be produced. By addition of a dilution network, square waves with different amplitudes and periods can be performed, and with other channel structures, more complex waveforms such as sine and triangle waves can be produced.¹⁹ Although these types of devices rely on off-chip pressure sources to drive fluid flow and extra channel structures to achieve periodic waveforms, this type of mixing was recently used to investigate gene expression in yeast upon a periodic stimulation with glucose.¹⁹ The main disadvantage of both the pulse code modulation method and flow-encoded switching is the complex nature of the microfluidic designs. With the large number of channels used in these designs, there is an increased probability of channel fouling and clogging. A more ideal strategy would be to develop a robust and simple microfluidic method to generate temporal gradients.

There have been a few examples of simple designs used to produce time-varying gradients; however, the majority of these devices would be difficult to use with cellular perfusion as they utilized electroosmotic flow (EOF) to drive solutions which may damage biological cells.^{20, 21} Off-chip pumps²² and EOF pumps²³ have also been used, but typically require numerous channels to achieve the gradient, or to pump, which again, can be problematic. A more simple microfluidic device has been used for mixing two analytes for flow-injection analysis, but did not produce temporal gradients of concentrations.²⁴

We have developed a simple method to produce temporal gradients of concentration using two on-chip diaphragm pumps and applied this method to perfusion of islets of Langerhans. The pumping system was characterized by comparing the amplitudes of a series of sine and triangle waves to theoretical waveforms. This system was used to apply a series of glucose concentrations to a single islet of Langerhans while monitoring $[Ca^{2+}]_i$. Oscillations of

$[Ca^{2+}]_i$ were observed indicating that the islet responded normally and that this system will be useful in further studies aimed at elucidating the mechanisms involved in islet physiology.

Materials and Methods

Chemicals and Reagents

HNO₃, CaCl₂, NaOH, and NaCl were purchased from EMD Chemicals, Inc. (Gibbstown, NJ). MgCl₂, HF and Cosmic Calf Serum (CCS) were from Fisher Scientific (Pittsburgh, PA). KCl, fluorescein, tricine, and Type XI collagenase were from Sigma (St. Louis, MO). Fluo-4 acetoxymethyl ester (Fluo-4 AM), Pluronic F-127, RPMI 1640, and penicillin-streptomycin were from Invitrogen (Carlsbad, CA). All solutions were made with Milli-Q (Millipore, Bedford, MA) 18 MΩ deionized water.

All solutions used in the microfluidic device were composed of 10 mM CaCl₂, 125 mM NaCl, 1.2 mM MgCl₂, 5.9 mM KCl, and 25 mM Tricine, made to pH 7.4 with NaOH. This buffer was supplemented with either 100 μM fluorescein or 20 mM glucose when characterizing pumps or performing islet measurements, respectively.

Fabrication of Microfluidic Chips

The photomask consisted of two layers, a valve layer and a fluid layer, and was printed in negative on film. Fabrication of the device was performed as previously described with more details given in the Supplementary Information (SI).^{25,26} After etching, the first two valve seats of each pump were 1.085 mm × 0.585 mm × 40 μm (length × width × depth), while the third valve seat was 1.025 mm × 0.525 mm × 11 μm (length × width × depth). The mixing channel was 120 mm long, 230 μm wide and 93 μm deep with a cross sectional area of 0.00177 mm² and a volume of 2.1 μL. The cell chamber was 0.3 mm in diameter with a volume of 0.2 μL.

Detection

Detection was performed on the stage of a Nikon TS100F microscope. Light from a Xenon arc lamp (Intracellular Imaging, Inc., Cincinnati, OH) was coupled into the back of the microscope, made incident on a 40×, 0.6 NA objective after passing through an excitation filter (FF01-482/35-25, Semrock, Inc., Rochester, NY) and dichroic beamsplitter (FF506-Di02-25x36, Semrock). Fluorescence was collected by the same objective, passed through the dichroic and emission filter (FF01-536/40-25, Semrock) prior to passing into a microscope photometer (Photon Technology International, Inc., Birmingham, NJ). The photometer was used to visualize the detection region and allowed adjustment of a spatial filter to ensure fluorescence was being collected from the channel of interest before being detected by a photomultiplier tube (PMT). A thermofoil and thermocouple (Omega Engineering, Inc., Stamford, Connecticut) were attached to the microfluidic chip to maintain the temperature of the mixing channel and islet chamber at 37 °C.

Pumping design and program

A completed assembly device consisted of the microfluidic perfusion system held between a bottom and a top piece of polymethylmethacrylate (PMMA) by four machine screws. These PMMA pieces were fabricated in-house and facilitated air connections to the valve seats. Computer controlled valves (Model A00SC232P, Parker Hannifin Corp, Cleveland, OH) were used to apply vacuum and pressure to the device through the bottom PMMA piece. The two-piece manifold was fabricated such that it did not interfere with visualization or fluorescence measurements of the mixing channel and the cell chamber.

The sequence of opening and closing of the valves (inlet, diaphragm, and outlet valves) was similar to the original report with modifications.²⁵ Unless stated otherwise, 3 psi and 25 in Hg was applied to the valve seats to close and open the valves, respectively. In step 1, vacuum was applied to the inlet valve for 120 ms. In step 2, vacuum was maintained on the inlet valve and applied to the diaphragm valve for 120 ms. Step 3, pressure was used to close the inlet valve, while vacuum was kept on the diaphragm valve for 150 ms. The volume of liquid in the diaphragm valve at this time defined the volume displaced per pump cycle. In step 4, the diaphragm valve was closed and the outlet valve opened simultaneously and held for 210 ms. A 5th step was used to close all valves and the time of this step (the “idle time”) was varied as described below.

To dilute an analyte from pump A to a final percentage (x_A) of the initial concentration, the ratio of the flow rates from the two pumps was varied. The flow rates were varied by changing the time of the 5th step of each pump cycle, the idle time. Qualitatively, for a small value of x_A (a large dilution), fewer pump cycles per minute from pump A would be performed (a large idle time used per pump cycle); whereas more pump cycles from pump B would be used (a small idle time per pump cycle).

As described in the SI, a series of equations were developed to quantitatively define the idle time for pump A ($IT_{Pump\ A}$) and for pump B ($IT_{Pump\ B}$) as a function of x_A . The final equations used to determine the value of the idle times were:

$$IT_{Pump\ A} = 0.6 \left(\frac{1 - x_A}{x_A} \right) \quad 0 < x_A < 1 \quad (3)$$

$$IT_{Pump\ B} = 0.6 \left(\frac{x_A}{1 - x_A} \right) \quad 0 < x_A < 1 \quad (4)$$

The value of x_A was input into a LabView (National Instruments, Austin, TX) program. The program controlled the timing and actuation of the valve sequence through an analog-to-digital data acquisition card (PCI 6221, National Instruments). Thus, with a new value of x_A , a new idle time was calculated and used in the 5th step of the valve sequence. PMT data collection was performed at 50 Hz using the aforementioned data acquisition card. More details of the equations and programs used to control the pumps are given in the SI.

Mixing verification

To test mixing, pumps A and B were used to deliver calibrant solutions that had been made offline, through the device. Online mixing was verified by placing 100 μ M fluorescein in the reservoir for pump A and diluting online to concentrations of 0, 25, 50, 75 and 100 μ M. These values were reproduced 3 times followed by concentrations of 3, 5, 10, 15, 30, 60, 80, 95, and 97 μ M with each concentration held at least 2 min. These offline and online mixing experiments were repeated after the microfluidic device and PMMA manifold were completely disassembled and reassembled ($n = 3$). In all cases, detection was made at the end of the mixing channel, 3 mm from the cell chamber. All data is presented as the mean of the three replicates ± 1 SD.

Isolation of Islets of Langerhans

Islets of Langerhans were collected as previously described with further details given in the SI.²⁶ For $[Ca^{2+}]_i$ monitoring, 1.5 μ L of 4.56 mM Fluo-4 AM in DMSO and 1.5 μ L Pluronic

F-127 in DMSO were combined and transferred into 2 mL RPMI to produce a final Fluo-4 AM concentration of 3.4 μM . An islet was placed in this solution and allowed to incubate at 37 $^{\circ}\text{C}$, 5% CO_2 for 30 min. After incubation, the islet was washed in 3 mM glucose and transferred to the cell chamber under a stereomicroscope. All $[\text{Ca}^{2+}]_i$ traces were normalized to the initial fluorescence value (F_0) and plotted as F/F_0 .

Results and Discussion

To test the various hypotheses as to the causes of islet $[\text{Ca}^{2+}]_i$ oscillations or insulin secretory oscillations, it would be useful to have a system that can accurately control the amount of glucose delivered to an islet. For full automation, it should be possible to perfuse with a range of glucose concentrations with the ability to easily change the concentration in time; however, a simple system composed of a minimal number of channels and structures should also be utilized to reduce difficulties associated with fabrication and utilization of complex devices. To achieve the above criteria, a 3-layer device was developed with two integrated pumps to deliver a glucose solution and a buffer solution into a mixing channel, prior to pumping the diluted and fully mixed solution into a cell chamber where $[\text{Ca}^{2+}]_i$ was monitored using a fluorescent dye (Figure 1).

Reduction of backflow

The original sequence²⁵ of opening and closing the valves produced a flow back to the pumps, termed backflow, when the third valve was opened (step 4 in Figure 2A). This backflow could be observed when fluorescein was pumped through the device and the fluorescence intensity of the liquid head passed through the detection profile. As shown in Figure 2B, a pattern was produced as the fluorescence intensity increased followed by a sharp drop in the fluorescence. This pattern was repeated 3 times as the liquid head traversed the detection region and was due to the liquid head first moving into the detection region, causing the increase in fluorescence intensity, followed by the backflow, which removed fluorescein from the detection region and resulted in the subsequent decrease in fluorescence intensity. This effect has been observed elsewhere²⁷ and in some cases may not be problematic as the net displacement is still forward; however, backflow was undesirable for islet experiments, as pulsing of solutions may introduce artificial pulsing or oscillations in the islet.

To reduce backflow, the 4th and 5th step of the original sequence were combined into a single step (step 4, Figure 2C). With this modification, the diaphragm valve closed, pushing liquid out, simultaneously as the outlet valve opened, pulling solution in from the rest of the channels. As the third valve seat was etched more shallow (~5 nL) than the diaphragm valve (~20 nL), the amount of liquid pushed out by the diaphragm valve more than compensated for the volume pulled in by the third valve resulting in a net forward displacement for this combined step. With these modifications, backflow was negligible as no decrease in fluorescence intensity was observed when fluorescein was pumped through the detection region (Figure 2D).

Mixing verification

To produce dilutions, the flow rates from the two pumps were varied resulting in different ratios of analyte and buffer pumped into the mixing channel while maintaining a final total flow rate. The design required complete mixing in both lateral and longitudinal directions to achieve the desired output concentration; therefore, it was necessary to verify complete mixing had occurred in the mixing channel prior to further experiments. As shown in Figure S-1 and discussed further in the SI, mixing was shown to be complete in both lateral and longitudinal directions. Videos of the junction between pump A and B can also be found in the SI.

To ensure the correct final dilution was produced, 100 μM fluorescein was pumped from Pump A and diluted with buffer from Pump B at different ratios (Figure 3A). The production of multiple final concentrations were achieved by varying the value of x_A , in equation 3 and equation 4 to values of 0.00, 0.03, 0.05, 0.10, 0.15, 0.25, 0.30, 0.50, 0.60, 0.75, 0.80, 0.95, 0.97, and 1.00 which produced the corresponding changes in the idle times of the two pumps. The average intensity values of these solutions were compared to intensity values of standard solutions made off-chip and pumped through the device. Figure 3B summarizes these results and indicates that the concentrations produced by on-line mixing (open symbols) were comparable to the premixed solutions (closed symbols). Included in Figure 3B are results when this experiment was repeated twice more after the device and manifold had been disassembled and reassembled. As observed, the correct mixing ratios were attained between assemblies, indicating that the device could be removed from the detection system, cleaned or loaded with cells, and reassembled reproducibly. To demonstrate the stability of the online mixing, 30 μM fluorescein was produced and held for 35 min. The slope of the linear fit to this data was $-3.487 \times 10^{-6} \text{ V s}^{-1}$, demonstrating the ability to mix and maintain a reproducible concentration over a long period of time.

Flow rates were determined as explained in the SI. For the multiple assemblies shown in Figure 3A, the average flow rate was $1.43 \pm 0.07 \mu\text{L}/\text{min}$ (Figure S-2). The response time of the system, the time for the concentration to change from 10% to 90% of the final concentration upon a step change in x_A , was also measured from the data in Figure 3A. The average response time was $20.3 \pm 2.1 \text{ s}$ across all assemblies of the device and manifold.

Continuous gradient

To explore the ability of the device to generate temporal gradients and to characterize the pumping system, concentration waveforms in the form of sine and triangle waves were produced. In contrast to the step gradients shown above, these continuous gradients were achieved by changing the value of x_A in steps of 0.1% at various frequencies. Amplitudes are presented in % of the maximum signal (100 μM fluorescein) with a median amplitude of 50%. For example, a sine wave with amplitude of 25% indicates that the 100 μM fluorescein solution was diluted from 25 to 75 μM at a specified frequency.

Figure 4 shows 4 sine waves at 0.00245 Hz with amplitudes of 10%, 25%, 35%, and 40%. Three periods at each amplitude were performed. At approximately 1100 s, the wave was distorted because of an air bubble, but once the bubble passed through the device, the signal returned to expected values. To determine if the amplitudes of the generated waves matched the intensities of known solutions, fluorescein was mixed online at 5 different concentrations and the average PMT intensity values are shown as the dashed horizontal lines. As seen, the amplitudes of the generated sine waves match well to the online-mixed solutions.

Each wave at the various frequencies and amplitudes were compared to theoretical waves at the same values. Figure S-3 in the SI compares two generated curves to their theoretical curves. At low frequencies, the generated sine waves reached the correct amplitudes, however, at higher frequencies the sine waves did not. Triangle waves did not reach the correct amplitude at any of the frequencies tested. Differences between generated and theoretical curves could be due to broadening of the peaks from longitudinal diffusion, Taylor dispersion, and/or convective flows as they traveled through the mixing channel. Also, as mentioned in the SI, the current pump cycle must have finished before a new idle time was utilized. Thus, at low or high % amplitudes, when the pumps had large idle times, a new x_A value could not be used until the previous pump cycle was complete, thereby creating a phase shift in the output value from the theoretical value.

The ability of the device to produce continuous gradients was summarized by measuring the amplitude response. As seen in Figure S-4, the results indicated that continuous gradients in time were possible, although within a defined frequency and amplitude range. It may be possible to extend this range via altering the initial concentration of analyte in the reservoir. In addition, the lag time could be reduced which would reduce the amount of peak broadening and increase the frequency range of the device.

Stimulation of islets

To demonstrate that the system developed was suitable for utilization with islets of Langerhans, single islets were stimulated by glucose concentration gradients and changes in $[Ca^{2+}]_i$ were monitored. An islet was loaded into the device under non-stimulatory glucose concentrations (3 mM) and the Fluo-4 fluorescence recorded for 120 s before pumping commenced with 3 mM glucose. As shown by the thin dashed line in Figure 5A, the pumping action did not appear to have a large effect on the measured fluorescence except a small change attributed to fresh solution driven in by the pumps. This result was consistent for all islets tested ($n = 5$). During all islet experiments, the position of the islet within the spatial filter of the microscope photometer was verified after the pumping began to ensure the islet did not move out of the detection region. To verify, the islet was visualized which blocked the fluorescence to the PMT and resulted in the drop in signal at 240 s and 100 s in Figure 5A and 5B, respectively.

In total, 4 out of 5 islets responded to one of two glucose stimulatory profiles that were used. One of these profiles is shown in Figure 5A and consisted of a square wave of glucose concentration, from 3 mM to 11 mM and back to 3 mM. Based on the average flow rate and response time of the system, the time the new glucose concentration entered the cell chamber was estimated as 108.6 ± 5.3 s after the new glucose concentration was input into the program. This arrival time is shown as the bold dotted line in Figure 5A (~ 415 s) with the error expressed as the width of the line. The glucose concentration was held at 11 mM for 12 min to allow the dynamics of $[Ca^{2+}]_i$ to be observed. As shown, after approximately 15 s of elevated glucose, a decrease in the $[Ca^{2+}]_i$ was observed followed by oscillations with periods between 60 and 120 s. There are several features of this trace that matched features from other reports and provided evidence that the islet was responding in the correct physiological manner. First, the amount of time needed for the islet to respond to elevated glucose levels was similar to other reported values.^{28–31} Next, the decrease in $[Ca^{2+}]_i$ upon stimulation with glucose was likely due to the activation of Ca^{2+} -dependent enzymes upon glucose metabolism, as observed elsewhere.^{28–31} Third, the period of $[Ca^{2+}]_i$ oscillations were all within previously reported ranges.^{28–31} Finally, when the glucose concentration was returned to 3 mM, $[Ca^{2+}]_i$ levels returned to pre-stimulatory values indicating the Ca^{2+} responses were due to the increase in glucose concentration. It should be noted that the buffer used to stimulate the islets contained 10 mM $CaCl_2$ which is higher than typical physiological buffers. However, this concentration has been used before in other reports to ensure observation of slow $[Ca^{2+}]_i$ oscillations.^{6,28}

A second glucose profile was applied to other islets, with a representative trace shown in Figure 5B. Glucose concentration was increased in steps and included 3, 8, 12, and 20 mM with a final return to 3 mM. Each of these different glucose values produced different Ca^{2+} responses, with the trend that increased glucose concentrations resulted in increased periods of slow oscillations, until finally at 20 mM glucose there were only fast oscillations. The result in Figure 6B was similar to a theoretical model which modeled the $[Ca^{2+}]_i$ oscillations due to both glycolytic oscillations and electrical oscillations and showed that at high glucose concentrations, a loss of slow $[Ca^{2+}]_i$ oscillations would be observed.³²

Conclusion

A microfluidic perfusion chip was developed for investigating cellular dynamics. The waveforms of concentration produced with the device matched well with theoretical waveforms. To improve the amplitude response in the future, an active mixer may be employed which should reduce the time needed for mixing and the amount of longitudinal diffusion. By reducing the backflow to undetectable amounts, the device could be used in biological research. Monitoring of single islet $[Ca^{2+}]_i$ changes was successfully performed with results comparable to previously reported measurements and theoretical predictions.

The perfusion system should be suitable for a wide variety of cell types where a simple, all-chip perfusion system is needed. Besides monitoring $[Ca^{2+}]_i$, the chip can be coupled to additional analysis and detection units such as microfluidic separations for measurement of other physiological parameters. While a single output was demonstrated here, it should be possible to increase the throughput of the system by increasing the number of cell chambers. While the volumetric flow rate would be split among the outputs, with some modifications of this system, it should be possible to perfuse a larger number of islets in parallel.

Supplementary Material

Refer to Web version on PubMed Central for supplementary material.

Acknowledgements

This work was funded in part by grants from NIH R01 DK080714 and the American Heart Association Greater Southeast Affiliate.

References

1. Tornheim K. *Diabetes* 1997;46:1375–1380. [PubMed: 9287034]
2. Kennedy RT, Kauri LM, Dahlgren GM, Jung S-K. *Diabetes* 2002;51:152–161. [PubMed: 11756335]
3. Longo EA, Tornheim K, Deeney JT, Varnum BA, Tillotson D, Prentki M, Corkey BE. *J. Biol. Chem* 1991;266:9314–9319. [PubMed: 1902835]
4. Jung S-K, Aspinwall CA, Kennedy RT. *Biochem. Biophys. Res. Commun* 1999;259:331–335. [PubMed: 10362508]
5. Henquin J-C. *Diabetes* 2000;49:1751–1760. [PubMed: 11078440]
6. Gilon P, Henquin J-C. *Endocrinology* 1995;136:5725–5730. [PubMed: 7588329]
7. Matthews DR, Lang DA, Burnett M, Turner RC. *Diabetologia* 1983;24:231–237. [PubMed: 6345247]
8. O'Rahilly S, Turner RC, Matthews DR. *N. Engl. J. Med* 1988;318:1225–1230. [PubMed: 3283553]
9. Dertinger SK, Chiu DT, Jeon NL, Whitesides GM. *Anal. Chem* 2001;73:1240–1246.
10. Pihl J, Sinclair J, Sahlin E, Karolsson M, Petterson F, Olofsson J, Orwar O. *Anal. Chem* 2005;77:3897–3903. [PubMed: 15987089]
11. Lin F, Saadi W, Rhee SW, Wang S-J, Mittal S, Jeon NL. *Lab Chip* 2004;4:164–167. [PubMed: 15159771]
12. Wu H, Huang B, Zare RN. *J. Am. Chem. Soc* 2006;128:4194–4195. [PubMed: 16568971]
13. Irimia D, Geba DA, Toner M. *Anal. Chem* 2006;78:3472–3477. [PubMed: 16689552]
14. Amarie D, Glazier JA, Jacobson SC. *Anal. Chem* 2007;79:9471–9477. [PubMed: 17999467]
15. Shackman JG, Dahlgren GM, Peters JL, Kennedy RT. *Lab Chip* 2005;5:56–63. [PubMed: 15616741]
16. Rocheleau JV, Walker GM, Head WS, McGuinness OP, Piston DW. *Proc. Natl. Acad. Sci. USA* 2004;101:12899–12903. [PubMed: 15317941]
17. Azizi F, Mastrangelo CH. *Lab Chip* 2008;8:907–912. [PubMed: 18497910]
18. King KR, Wang S, Jayaraman A, Yarmush ML, Toner M. *Lab Chip* 2008;8:107–116. [PubMed: 18094768]

19. Bennett MR, Lee Pang W, Ostroff NA, Baumgartner BL, Nayak S, Tsimring LS, Hasty J. *Nature* 2008;454:1119–1122. [PubMed: 18668041]
20. Kutter JP, Jacobson SC, Ramsey JM. *Anal. Chem* 1997;69:5165–5171.
21. Broyles BS, Jacobson SC, Ramsey JM. *Anal. Chem* 2003;75:2761–2767. [PubMed: 12948147]
22. Brennen RA, Yin H, Killeen KP. *Anal. Chem* 2007;79:9302–9309. [PubMed: 17997523]
23. Lazar IM, Karger BL. *Anal. Chem* 2002;74:6259–6268. [PubMed: 12510747]
24. Leach AM, Wheeler AR, Zare RN. *Anal. Chem* 2003;75:967–972. [PubMed: 12622393]
25. Grover WH, Skelley AM, Liu CN, Lagally ET, Mathies RA. *Sens. Actuators B* 2003;89:315–323.
26. Roper MG, Shackman JG, Dahlgren GM, Kennedy RT. *Anal. Chem* 2003;75:4711–4717. [PubMed: 14674445]
27. Inman W, Domansky K, Serdy J, Owens B, Trumper D, Griffith LG. *J. Micromech. Microeng* 2007;17:891–899.
28. Gilon P, Arredouani A, Gailly P, Gromada J, Henquin J-C. *J. Biol. Chem* 1999;274:20197–20205. [PubMed: 10400636]
29. Westerlund J, Bergsten P. *Diabetes* 2001;50:1785–1790. [PubMed: 11473039]
30. Antunes CM, Salgado AP, Rosario LM, Santos RM. *Diabetes* 2000;49:2028–2038. [PubMed: 11118004]
31. Fox JE, Gyulkhandanyan AV, Satin LS, Wheeler MB. *Endocrinology* 2006;147:4655–4663. [PubMed: 16857746]
32. Bertram R, Sherman A, Satin LS. *Am. J. Physiol. Endocrinol. Metab* 2007;293:890–900.

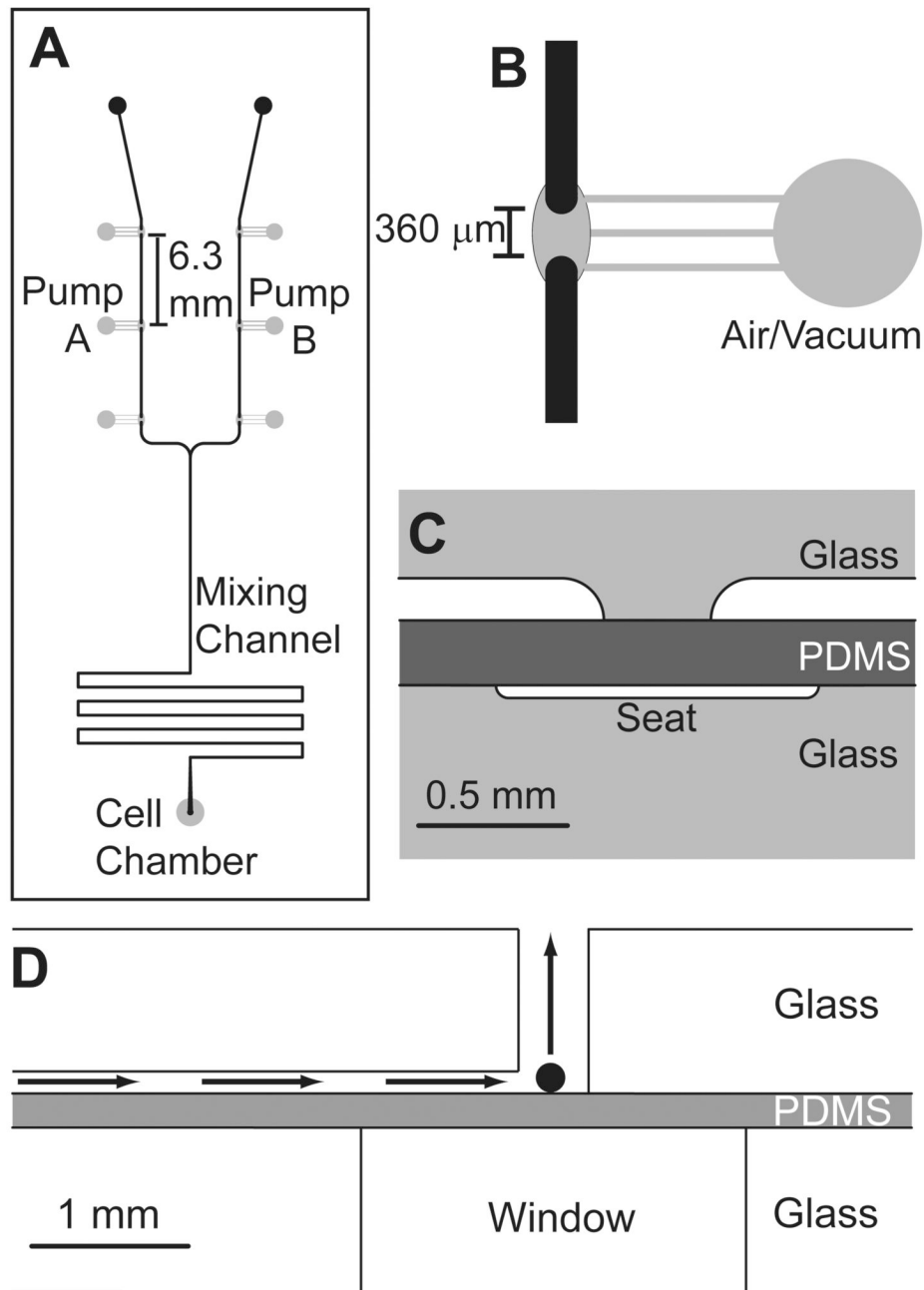


Figure 1. Microfluidic perfusion system

A. Top view of the microfluidic design used in the experiments. Pump A and B were operated at varying flow rate ratios to deliver varying concentrations of a stimulant and a diluent, respectively, into a mixing channel while maintaining a constant total flow rate. The valving channels are shown in grey and were fabricated in the bottom piece of the 3-layer device. Fluid channels are shown in black and fabricated in the top layer. **B.** A zoomed-in view of a valve. The discontinuous region of the fluid channel was $360\ \mu\text{m}$ after etching. **C.** Side view of the valve in the 3-layer device. Vacuum or air was applied to the valve seats, which pushed and pulled the PDMS layer, respectively, opening and closing the valve. **D.** Side view of the cell chamber. The black sphere is representative of a $100\ \mu\text{m}$ diameter islet of Langerhans within

the 300 mm diameter cell chamber. The perfusion direction is given by the arrows. The window below the islet facilitated fluorescence monitoring of intracellular Ca^{2+} changes. All figures are drawn to scale.

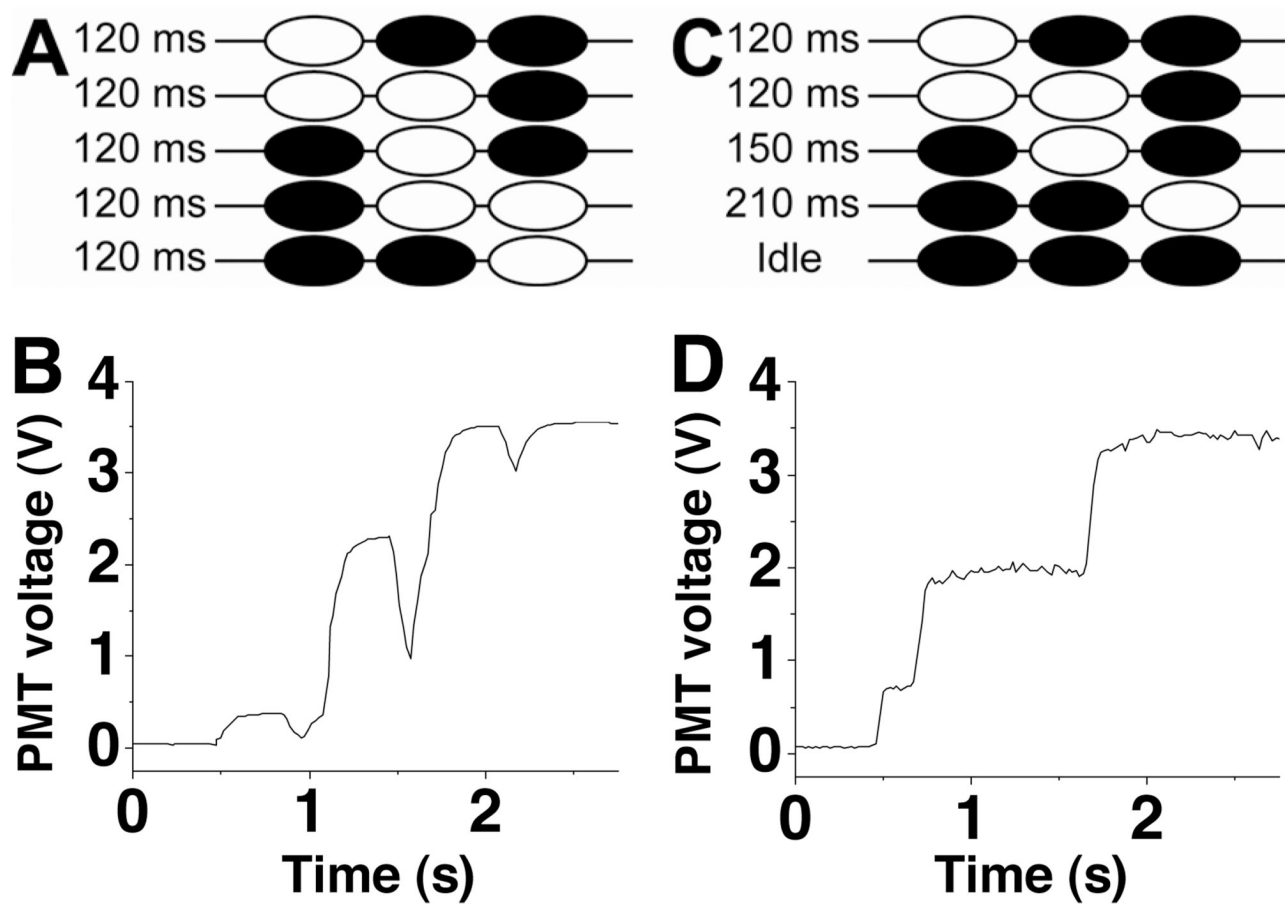
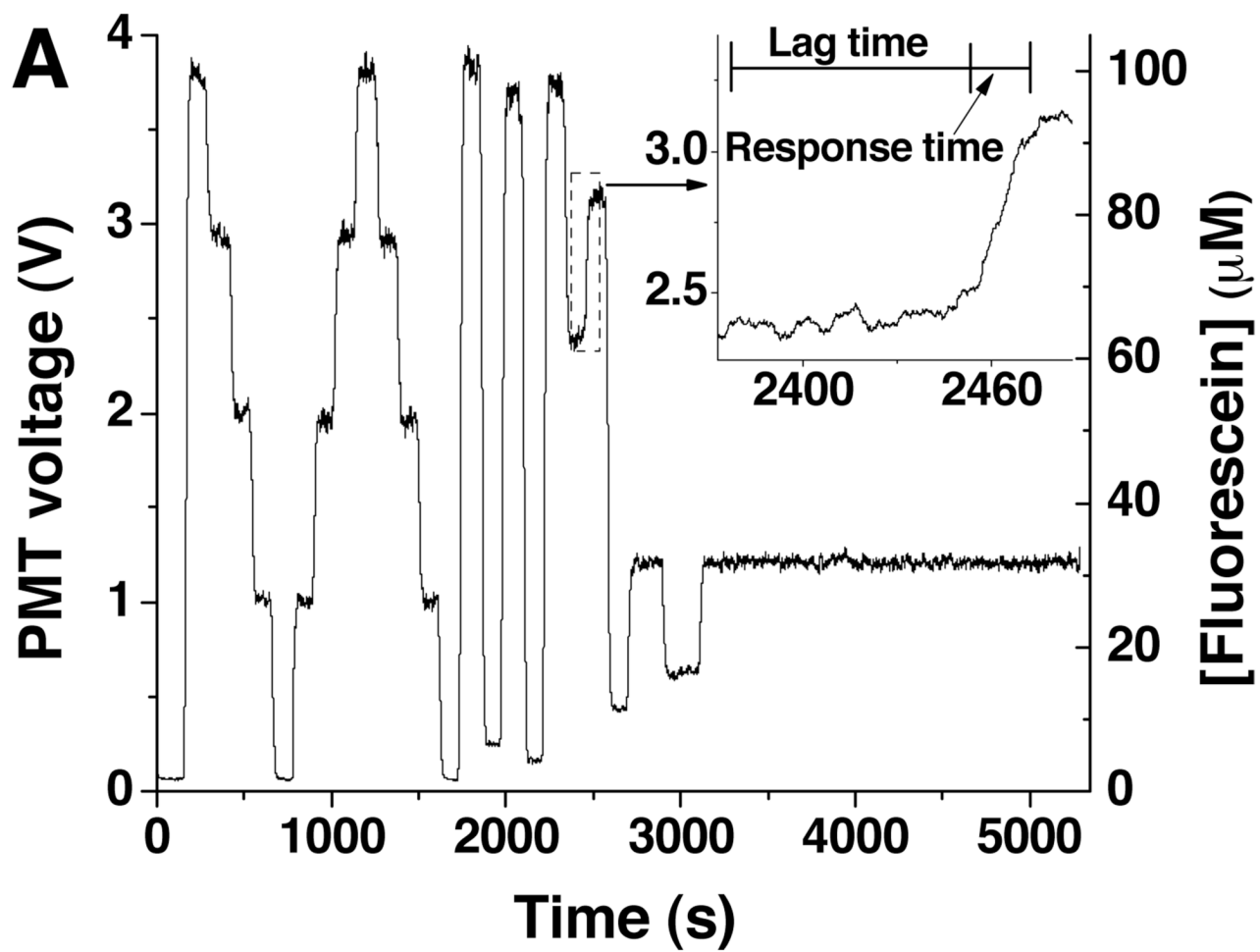


Figure 2. Reduction of backflow

A. Valving sequence using the original sequence of opening and closing the valves (from reference²⁵). White and black valves indicate open and closed valves, respectively. **B.** Using the valving sequence described in A, the fluorescence intensity of fluorescein was pumped through the detection region. Decreases at 1 s, 1.6 s, and 2.1 s were due to backflow. **C.** The new pumping sequence shown with the same coloring scheme as in A. **D.** Using the valving sequence described in C, the fluorescence from fluorescein pumped through the detection region is shown.



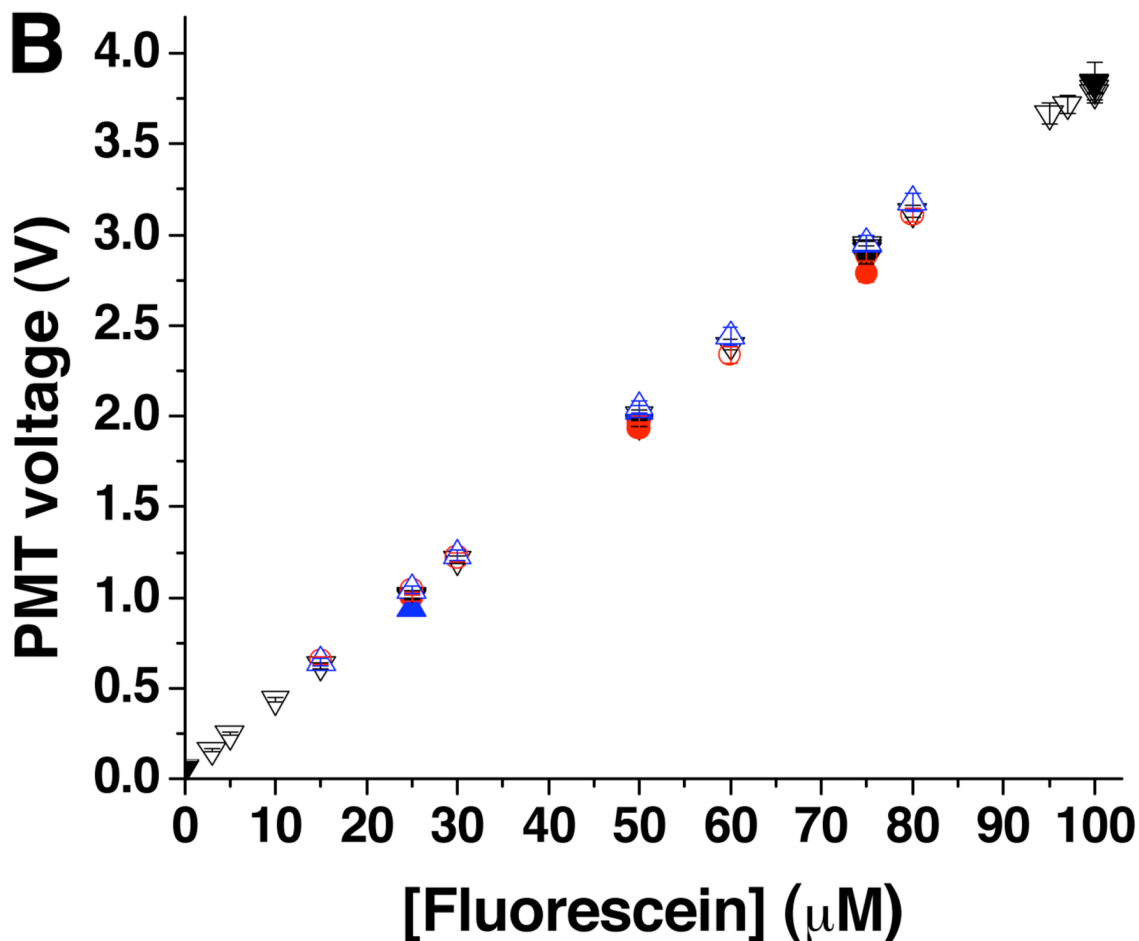


Figure 3. Online-mixing of fluorescein

A. Online mixing of 100 μM fluorescein was performed to produce final concentrations of 0, 25, 50, 75, and 100 μM fluorescein ($n = 3$) followed by dilutions to 3, 5, 10, 15, 30, 60, 80, 95, and 97 μM . The inset shows the time course of the change from 60 to 80 μM . The times corresponding to the lag and response time are indicated. **B.** Average PMT readings for each of the different online-mixed concentrations (open symbols) were plotted against the intended final concentration. Offline-mixed fluorescein solutions at concentrations of 0, 25, 50, 75, and 100 μM are plotted on the same graph (closed symbols). Shown on this graph are the results of three assemblies of the microfluidic device and PMMA manifold corresponding to black, blue, and red symbols.

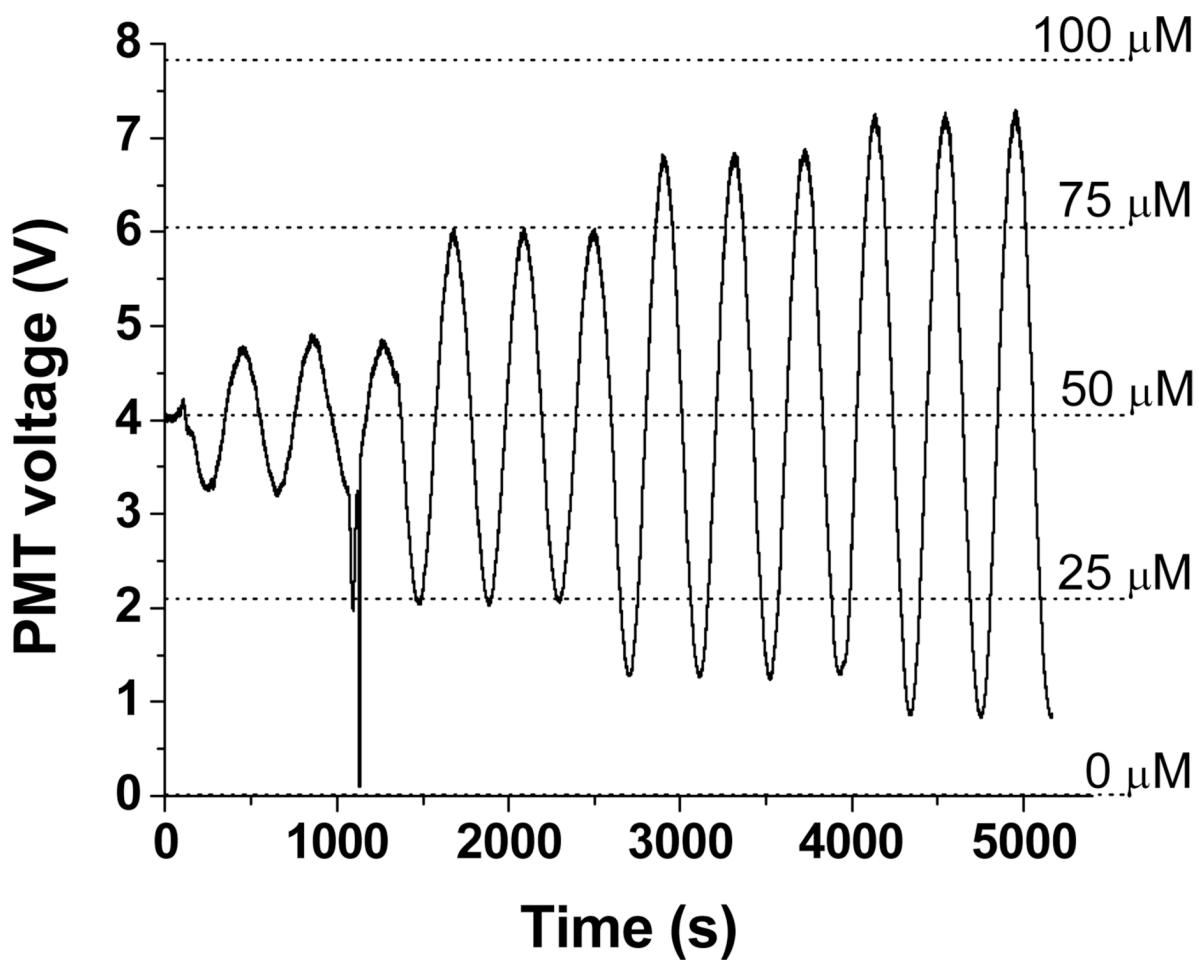


Figure 4. Continuous gradient generation

Sine waves were generated at 0.00245 Hz with amplitudes of 10%, 25%, 35%, and 40%. The 5 dashed lines show the fluorescence intensities of standard solutions of 0, 25, 50, 75, and 100 μM fluorescein.

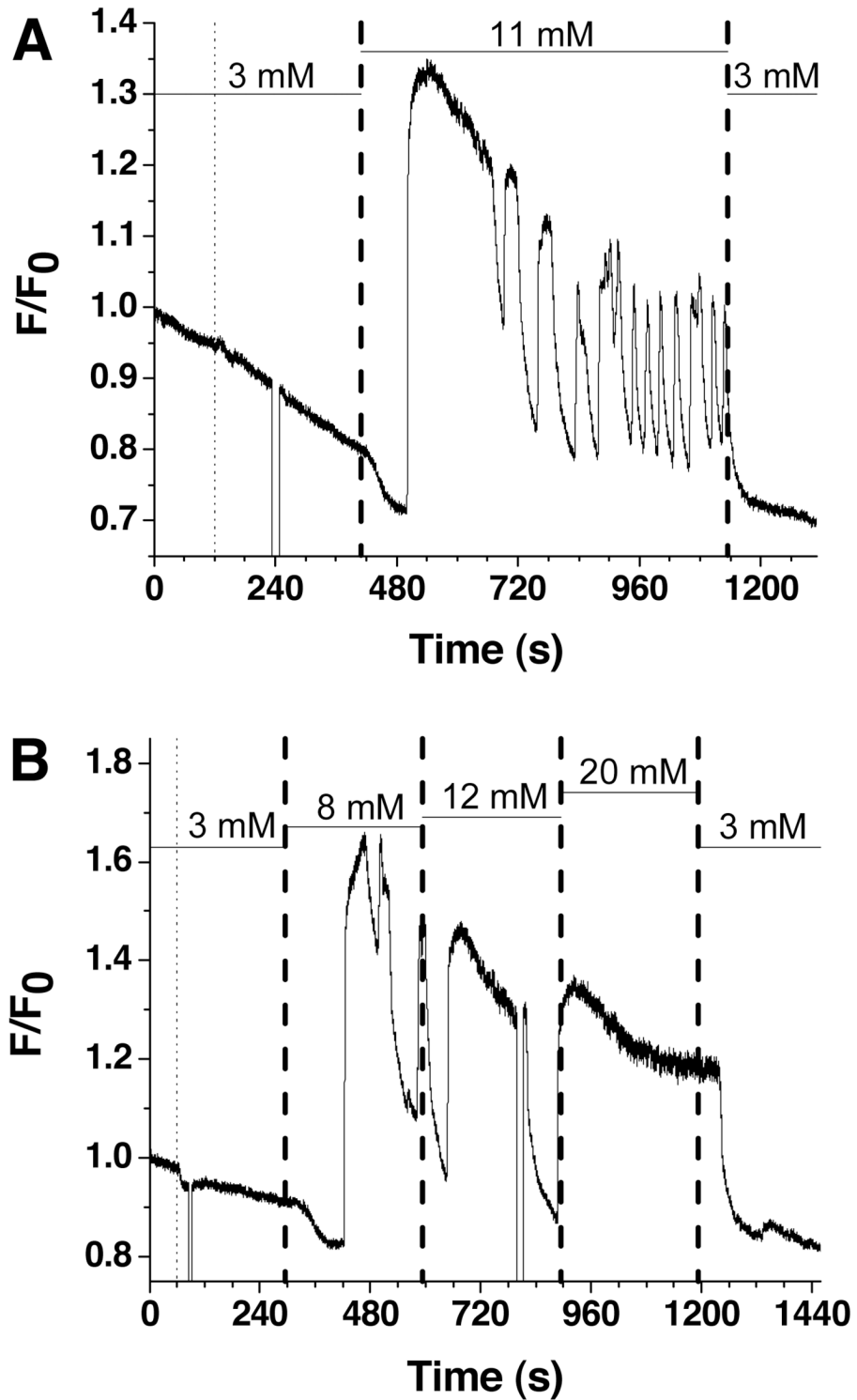


Figure 5. Single islet $[Ca^{2+}]_i$ responses to glucose stimulation

A. Fluo-4 fluorescence from a single islet was measured as a function of time in response to a single step change in glucose concentration. The glucose concentration in the perfusion system

was changed as shown by the horizontal bars above the fluorescence trace. The thin dashed line represents the time the pumping commenced while the thick dashed line indicates the time the glucose entered the cell chamber as estimated by the average flow rate and response time of the system. The error in the flow rate and response time measurements is shown by the thickness of the dashed lines. **B.** A second glucose waveform was applied in steps from 3, 8, 12, 20, and back to 3 mM.